



# Highly dispersed Pt on B<sub>2</sub>O<sub>3</sub>/Al<sub>2</sub>O<sub>3</sub> support: catalytic properties in the total oxidation of 1-butene

Robert E. Przekop<sup>1</sup> · Piotr Kirszensztejn<sup>1</sup>

Received: 16 January 2016 / Accepted: 18 February 2016 / Published online: 2 March 2016  
© The Author(s) 2016. This article is published with open access at [Springerlink.com](http://Springerlink.com)

**Abstract** Applying a newly proposed method for the synthesis of a binary system Al<sub>2</sub>O<sub>3</sub>/B<sub>2</sub>O<sub>3</sub>, a series of metal phase supports with the ratio of B:Al components varied in the range from 0.05 to 1 was obtained. The supports were loaded with a metal phase from the water solution of H<sub>2</sub>PtCl<sub>6</sub> to get the final load of 1 % of the metallic phase. The samples were subjected to thermal treatment under oxidizing or reducing conditions. The degree of dispersion of the metal phase, evaluated on the basis of hydrogen chemisorption, was very high, reaching a maximum of over 150 %. The catalytic performance of the catalysts was tested in the reaction of temperature-programmed complete oxidation of 1-butene.

**Keywords** Nanometals · Supports · 1-Butene oxidation · Chemisorption · Highly dispersed Pt

## Introduction

As indicated by recent literature reports [1], the catalytic centers related to the atomically dispersed noble metals can be considered in the aspect of metal interacting with the surface ligand present on the surface of a solid support. This consideration can be applied both to uniform crystalline structures, e.g. zeolites, as well as to oxide supports. The possibility of noble metal existence (i) under difficult reaction conditions, (ii) on easily reducible oxide supports (e.g. cerium oxide), in the form of subnanometric clusters (iii) or in atomic dispersion has brought about a new approach to Taustner's idea of strong

---

**Electronic supplementary material** The online version of this article (doi:[10.1007/s11144-016-1006-9](https://doi.org/10.1007/s11144-016-1006-9)) contains supplementary material, which is available to authorized users.

---

✉ Robert E. Przekop  
r.przekop@gmail.com; rprzekop@amu.edu.pl

<sup>1</sup> Faculty of Chemistry, A. Mickiewicz University, Umultowska 89b, 61-614 Poznan, Poland

interaction between the metal and cluster support [2, 3]. The cations of platinum, palladium, rhodium or other metals, anchored to the support through the M–O bonds can form in the configurations that are stable and catalytically active in a few reactions, in particular, oxidation and reduction. It is expected that development of effective methods for the synthesis and identification of suitable stabilizers and promoters will bring an increased range of cost-effective applications of atomically dispersed noble metal based catalysts. In heterogeneous catalysis, the distribution of active centers in which individual atoms or clusters of atoms are catalytically active can be compared to the molecular catalysis in a homogeneous catalytic system, which can grow links between these two types of catalysis. A binary oxide system,  $\text{Al}_2\text{O}_3/\text{B}_2\text{O}_3$ , has been applied in many reactions based on the use of heterogeneous catalysts. Thanks to its acidity, this system can be used in the reactions of Beckmann rearrangement [4–10], alcohol dehydration [11–14], partial oxidation of olefins [15–19], cracking [20–23], isomerization of hydrocarbons [24, 25] and toluene disproportionation [25, 26]. On the other hand, this system proved to be an effective support of metallic phase active in a number of reactions important for industry, like in the reactions of metathesis where it was a support of rhenium [27, 28], cyclohexene hydrogenation, where it was a support of platinum [29] or carbon oxide hydrogenation as a support of ruthenium [30]. The versatile character and multifunctional applications of this support are related to its specific acidic properties. It is known that the catalytic activity of platinum on oxide support depends to a considerable degree on the strength of acidic centers or on the general acid–base character of the support. Moreover, not only the activity but also the degree of dispersion significantly increases with increasing acidity of the support. Yazawa et al. [31], on the basis of interpretation of the XANES spectra of the catalysts: Pt/SiO<sub>2</sub>, Pt/Al<sub>2</sub>O<sub>3</sub>, Pt/MgO, have shown that for the supports of basic character under oxidizing conditions, platinum has an increased tendency towards occurrence in oxidized states. As a consequence, the degree of its dispersion decreases and its activity in the reactions of oxidation or total combustion decreases. The literature provides many reports on the reduced activity of platinum in the reactions of hydrocarbon combustion, in the presence of surface forms of PtO<sub>x</sub>. This phenomenon is related to a greater mobility of this phase on the surface of oxide supports, leading to coalescence of Pt.

The main aim of the study was to design a binary system  $\text{Al}_2\text{O}_3\text{--B}_2\text{O}_3$  to be a support for a catalyst with a metal (Pt) phase. In view of the earlier studies performed on similar binary gels [32–36] with Al<sub>2</sub>O<sub>3</sub> or SiO<sub>2</sub> as a matrix, a similar approach was applied in the design and synthesis of a catalyst with metal phase. The proposed method for the synthesis of a binary oxide support based on employing sol–gel processes, permitted the elimination of the presence of inorganic additives that could obscure the process of interaction between the metal phase precursor and the support surface.

## Experimental

### Synthesis

The supports of the metal phase were the samples of grain size from 0.1 to 0.2 mm, obtained according to the procedure described in [34, 35]. The precursor of the

metal phase was a standard water solution of hexachloroplatinic acid [ $\text{H}_2(\text{PtCl}_6)$ ] containing 14.28 g Pt/dm<sup>3</sup>. Proper amounts of the solution were deposited on the surface of gel support by the method of incipient wetness impregnation, then the samples were dried in a vacuum evaporator at 100 °C for 8 h. The precursor was transformed to the metal phase by thermally programmed reduction in  $\text{H}_2$  atmosphere, on temperature increasing at the rate of 5°/min, with 10 min plateaus at 100 and 200 °C and a 180 min plateau at 250 °C. The final temperature of annealing was 500 °C at which the samples were kept for about 60 min. The process of cooling to 200 °C was also performed in  $\text{H}_2$  atmosphere, which was afterwards replaced by 99.99 % He as a cooling medium and continued to room temperature. The catalyst loading with metal phase was the same in all samples and equal to 1 weight percent (wt%).

### Surface area

The surface area was determined by the low temperature (77 K) nitrogen adsorption measurements carried out on the Accelerated Surface Area and Porosimetry System model 2010 V2.00 D made by Micromeritics, using 200–300 mg of the support with the grain size fraction between 0.1 and 0.2 mm. Prior to nitrogen adsorption, all samples were outgassed at 623 K (350 °C) at 0.4 Pa till constant weight. Both the adsorptive and desorptive branches of the isotherm were taken in the range of  $p/p_0$  0–1.

### IR spectroscopy

Spectroscopic studies were carried out in a Bruker IFS 66 vacuum infrared spectrometer. The sample was placed in a water cooled cuvette, enabling a heat treatment up to 800 °C. The sample was heated at 750 °C under low pressure ( $10^{-3}$  mmHg) for 1 h before measurement. 10  $\mu\text{l}$  of  $\text{D}_2\text{O}$  was added to adsorb on the sample surface prior to sequence of thermal desorption at 300 °C (II), 450 °C (II), 600 °C (II), 750 °C (II) for 30 min ( $10^{-3}$  mmHg vacuum) and spectra measurement.

### Metal dispersion

Chemisorption experiments using hydrogen were performed at 35 °C in a Micromeritics ASAP (*Accelerated Surface Area and Porosimetry System*) model 2010 V2.00 D equipped with a chemisorption controller station. The procedure of  $\text{H}_2$  chemisorption on the samples obtained after thermally programmed reduction included degassing ( $10^{-5}$  mmHg) at 500 °C (1 h) followed by annealing in  $\text{H}_2$  atmosphere for 1 h at 500 °C and repeated degassing for 2 h at 500 °C. After these processes, the samples were cooled to 35 °C at which hydrogen was adsorbed. After the first adsorption, the samples were degassed for 2 h at 35 °C and then hydrogen was adsorbed again in order to establish the amount of weak adsorbed hydrogen. The difference in measurements 1 and 2 provided information on the amount of strongly chemisorbed hydrogen. The degree of dispersion was calculated assuming

that the stoichiometry of adsorption is 1 hydrogen atom per 1 platinum atom. For the system BA1 0.4, measurements of adsorption were also performed at 100 and 200 °C under the same activation conditions.

### Catalytic combustion of 1-butene

The activities of catalysts obtained were tested in the reaction of oxidation of 1-butene to CO<sub>2</sub>, which was performed according to the rules of thermally programmed reactions (TPRe) [37]. The reaction system included a Pfeiffer gas analyzer *ThermoStar*, model *GSD 301 T2*, with a *QMA 200 M* mass analyzer and a Faraday trap used as a detector, for the mass range: 1–200 amu. Analysis of the reaction gases was made with the use of the software *Pfeiffer Vacuum Quadstar*. The contents of CO<sub>2</sub>, C<sub>x</sub>H<sub>y</sub> and H<sub>2</sub>O were measured. The carrier gas and oxidizing agent was air. The stream of carrier gas dried on the adsorption column packed with zeolite 4A and 1-butene were directed to the mixer. The composition of the reactor feed was controlled by mass flow controllers. The concentration of 1-butene in the carrier gas (air) was 2000 ± 100 ppm. The internal diameter of the fixed-bed reactor was 6 mm. A portion of 60 mg of the catalyst was placed in a glass microreactor, a stream of the reaction mixture was fed on it and the temperature program was started. The rate of temperature increase was 20 °/min and the progress of reaction was recorded in the temperature range 308–673 K (35–400 °C). After the completion of the first measurement, the catalyst was cooled to 308 K (35 °C) in the reaction mixture stream containing 1-butene. After reaching 308 K (35 °C), the catalyst sample was subjected to the same procedure in combustion of 1-butene for the second time (followed activation).

### Electron microscopy

Transmission electron microscopy images were taken on a microscope TEM JEOL 200 CX made by Jeol. The images were recorded using the anode voltage of 80 kV. The processing, image analyses and crystallites size measurements were made using the program Gwyddion (GPL).

### Discussion

The ability to control the dispersion of precious metals (e.g., Pt, Pd) supported on oxide surfaces is a primary goal of the catalysts design and may lead to understanding the nature of metal-support interaction. The dispersion of these metals on the oxide supports is a critical factor because of the high cost of noble metals. As follows from the data presented in Table 1, for almost all binary oxide systems obtained (B<sub>2</sub>O<sub>3</sub>/Al<sub>2</sub>O<sub>3</sub>), the dispersion of Pt (H/Pt) was higher than in the system Pt/Al<sub>2</sub>O<sub>3</sub>, for which the degree of platinum dispersion determined on the basis of hydrogen chemisorption H/Pt was 1.07. It should be noted that the changes in the degree of dispersion of the metal phase is very similar to that of changes in the surface area, depending on the content of the boria containing component (B<sub>2</sub>O<sub>3</sub>) in

**Table 1** Changes in the degree of Pt dispersion and changes in the surface area as a function of the B/Al molar ratio

Symbol	Molar ratio		A Pt dispersion	B S <sub>BET</sub> (m <sup>2</sup> /g)
	B <sub>2</sub> O <sub>3</sub>	Al <sub>2</sub> O <sub>3</sub>		
B/Al 0.05	0.05	1.0	1.05	432
B/Al 0.1	0.1	1.0	1.24	528
B/Al 0.2	0.2	1.0	1.44	515
B/Al 0.3	0.3	1.0	1.64	526
B/Al 0.4	0.4	1.0	1.50	448
B/Al 1.0	1.0	1.0	0.98	317

Experimental conditions: Pt Dispersion (A)—degassing (10<sup>-5</sup> mmHg) 1 h 500 °C, annealing in H<sub>2</sub>, 1 h, 500 °C, repeated degassing, 2 h, 500 °C. Surface area (B) adsorption at 77 K, 200–300 mg of support, grain size 0.1–0.2 mm, outgassed at 623 K (350 °C) at 0.4 Pa

the Al<sub>2</sub>O<sub>3</sub> matrix (Table 1). The values of surface area S<sub>BET</sub> and the degree of metal phase dispersion (H/Pt) are higher for B<sub>2</sub>O<sub>3</sub>/Al<sub>2</sub>O<sub>3</sub> than for the support not modified with boria, and these values increase to reach a maximum for the sample of B/Al molar ratio of 0.3. A clearly visible correlation between these values evidences that the metal phase dispersion depends on the surface area (geometry) of the support.

For significant changes in the surface area of the systems studied (for Al<sub>2</sub>O<sub>3</sub> gel the surface area is 337 m<sup>2</sup> g<sup>-1</sup>, while for the samples of B/Al 0.1, 0.2 and 0.3, it is above 500 m<sup>2</sup> g<sup>-1</sup> [35] and the only sample with the highest content of B<sub>2</sub>O<sub>3</sub> (B/Al 1.0) has a slightly lower surface area (317 m<sup>2</sup> g<sup>-1</sup>), which is associated with the process boria of crystallization) more informative is presentation of the metal phase area (Pt), determined on the basis of H<sub>2</sub> adsorption isotherm, expressed per a unit area of the support, as shown in Fig. 1.

In general, the character of changes in the normalized area of Pt per 1 m<sup>2</sup> of the support taking place in response to increasing contribution of B<sub>2</sub>O<sub>3</sub> in the Al<sub>2</sub>O<sub>3</sub> matrix is very similar to that of changes in Pt dispersion degree shown in Table 1.

It should be noted that for sample B/Al 1.0, the values of Pt area per 1 m<sup>2</sup> of the support are similar to those obtained for sample B/Al 0.3. Taking into account the fact that the surface areas of these two samples differ by over 200 m<sup>2</sup> g<sup>-1</sup> (that of the sample with a lower content of boron was larger), it can be supposed that development of surface area of the support (depending on the content of boria) was not the main factor determining the relatively high amount of chemisorbed H<sub>2</sub>. This is illustrated in Fig. 1 by a large area of Pt per 1 m<sup>2</sup> of the support for the sample with the highest content of B<sub>2</sub>O<sub>3</sub> (B/Al = 1.0).

It is well known that the interaction of Pt particles with the oxide support can alter the electronic properties of the Pt and play a crucial role determining the particle morphology and maintaining the dispersion of Pt. For example, high dispersion can be achieved by specific interaction between defect sites on the support surface [38]. On the other hand, it has been confirmed that platinum on acidic supports is more electron-deficient than that on basic ones [39, 40] and platinum on the acidic support material is less oxidized than that on the basic one.

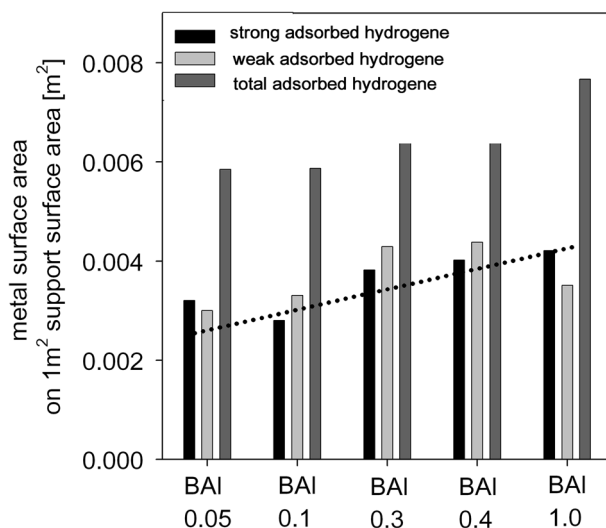


**Fig. 1** The normalized area of Pt per  $1 \text{ m}^2$  of the support determined on the basis of strongly and poorly adsorbed hydrogen  $\text{H}_2$ . Experimental conditions: degassing ( $10^{-5}$  mmHg) 1 h  $500^\circ\text{C}$ , annealing in  $\text{H}_2$ , 1 h,  $500^\circ\text{C}$ , repeated degassing, 2 h,  $500^\circ\text{C}$  After the 1st adsorption, cooled to  $35^\circ\text{C}$  and degassed ( $10^{-5}$  mmHg) 2 h,  $35^\circ\text{C}$  and 2nd was taken

Analysis of the crystallite size of the metal phase (Pt) in the TEM images recorded confirmed a high dispersion, or indicated that the metal phase occurs as a monolayer on the surface of the support. Very small crystallites of platinum can be identified in the TEM images, in contrast to their presence in the analogous gel systems  $\text{Al}_2\text{O}_3/\text{SnO}_2$  or  $\text{Al}_2\text{O}_3/\text{GeO}_2$  system (Supplementary Information). For these gel systems, Pt crystallites of the size from 8 to 90 nm were observed. Their size was dependent on the composition of the support. For the systems with a smaller content of  $\text{SnO}_2$ , e.g.  $\text{Sn}_g$  0.2 (Fig. 4e), the crystallites are smaller, of the size from 8 to 25 nm, while for the sample  $\text{Sn}_g$  1.0 (molar ratio  $\text{SnO}_2:\text{Al}_2\text{O}_3$  of 1:1), they are much greater, of the size 40–90 nm. For the systems modified with germanium(IV) oxide, the dispersion was much smaller than for the systems modified with  $\text{B}_2\text{O}_3$  and did not exceed 10 %. Increased dispersion was achieved only for the sample with a small content of  $\text{GeO}_2$  (molar ratio of  $\text{Ge}/\text{Al} = 0.05$  at the Pt loading up to 0.5 wt%); for this sample, the dispersion reached about 23 % and the Pt crystallites reached  $\sim 40$  nm.

The dispersion values obtained for the samples  $\text{B}_2\text{O}_3\text{--Al}_2\text{O}_3$  of over 100 % are contradictory to the theoretically possible maximum dispersion of the metal. The error of chemisorption measurements for the systems  $\text{H}/\text{Pt}$ ,  $\text{O}/\text{Pt}$  and  $\text{CO}/\text{Pt}$  can reach up to 10 % [41] so these results cannot be explained by the instrumental error. The measurements were repeated after a few months and confirmed the earlier obtained values with the maximum deviation of 4 %. The results of  $\text{H}_2$  chemisorption at elevated temperatures (Fig. 2) reveal that the higher the electron deficiency of the support (the more acidic it is), the stronger the bonds with the surface Pt atoms. For small metal clusters made of 2–20 atoms, the energy

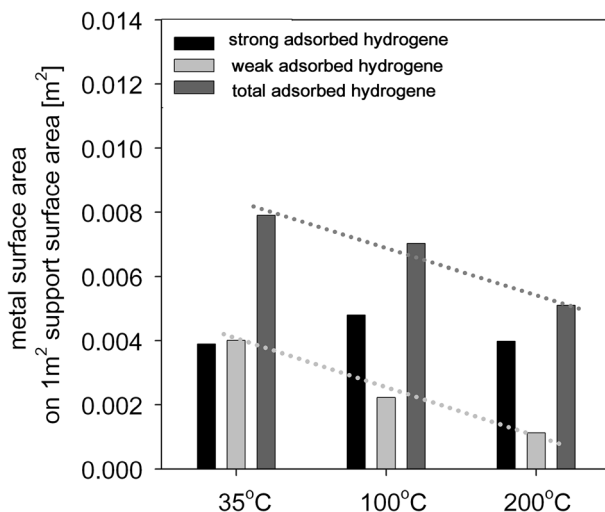


**Fig. 2** The effect of temperature on the amount of chemisorbed hydrogen for sample BAI 0.4. Experimental conditions: degassing ( $10^{-5}$  mmHg) 1 h 500 °C, annealing in  $H_2$ , 1 h, 500 °C, repeated degassing, 2 h, 500 °C. The 1st adsorption at 35, 100 and 200 °C. After the 1st adsorption degassed ( $10^{-5}$  mmHg) 2 h, 35, 100 and 200 °C and the 2nd was taken

of H/Pt bonding is much higher than that for the atoms of surface crystallites of the size greater than 2 nm [42], and the atoms at the vertices, and edges of the clusters show increased ability of  $H_2$  molecule adsorption. According to the theoretical calculations based on the Hückel model, for the clusters from  $Pt_2$  to  $Pt_{13}$ , the value of  $H/M_{max}$  varies from 5 to 1.9 [43].

The supports obtained containing boron oxide show much higher acidity and have strong acidic Brønsted type centers, whose presence was excluded for the reference systems  $SnO_2$  and  $GeO_2$ . On the other hand, an additional factor leading to the high dispersion of the metal phase and its stabilization is the matching of sizes of the metal crystallites to the pores in the oxide support. This hypothesis put forward in the 1950s by Boreksov [44] has attracted renewed interest and confirmation [45].

For Pt supported on  $Al_2O_3/SnO_2$ , it is difficult to relate the drastic decrease in Pt dispersion with mean size of pores on the support surface (Fig. 3). It can be supposed that for the easily reducible component  $SnO_2$ , the reason for reduced dispersion of Pt is formation of alloys of Pt with Sn. For the samples modified with boron oxide, there is a correlation between the degree of dispersion and the mean size of pores (Fig. 3). With decreasing pore diameter, the degree of dispersion increases. Of course, it is not possible to conclude from the above about the dominant role of this mechanism of stabilization, but it cannot be disregarded when considering the full spectrum of interactions.

Gel formulations containing  $B_2O_3$  are difficult to study in infrared spectroscopy (area “cut-of” below  $1600\text{ cm}^{-1}$  and have broad unresolved band stretching vibration of hydroxyl or hydrogen bond linked to the associates). Thus, the use of

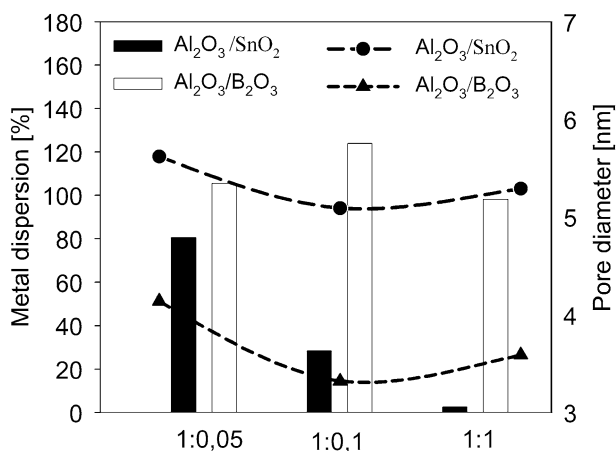


**Fig. 3** A comparison of the degree of Pt dispersion and the diameter of pores in the support for binary systems

molecular probes is in most cases difficult or impossible. On the other hand, the transmission IR spectrum of the binary oxide systems (subjected to a dehydration and dehydroxylation at temperatures above 500 °C) indicate that the surface of only the hydroxyl groups are bonded to the boron (3685–3693  $\text{cm}^{-1}$ ). D<sub>2</sub>O adsorption on this surface leads to the bandwidth derived from stretching vibration of O–D (2723  $\text{cm}^{-1}$ ) resulting from the adsorption of D<sub>2</sub>O to the Lewis acid centers (Fig. 4). Taking into account that boric acid (formed by the reaction of B<sub>2</sub>O<sub>3</sub> with H<sub>2</sub>O/D<sub>2</sub>O) is exclusively monobasic acid that acts not as a proton donor, but as a Lewis acid accepting OD<sup>−</sup>, it can be assumed that these groups are associated with exposed surface boron ions.

Taking into account that the catalytic reaction of hydrocarbons combustion is very important from the technological viewpoint for production of energy, the test reaction chosen was combustion of 1-butene. The reaction of full combustion of 1-butene permitted evaluation of the effect of addition of boron oxide on the activity of catalysts with supported metal phase, on the basis of measurement of temperature at which full conversion of 1-butene is observed for a given catalyst.

With increasing content of B<sub>2</sub>O<sub>3</sub> in the support, the temperature of maximum conversion of 1-butene decreases at first, reaching a minimum for sample Pt/BAI 0.3 and then increases. The character of T<sub>max</sub> changes is similar to that of the changes in Pt dispersion (H/Pt) presented in Table 1. It should be noted that the Pt catalysts supported on binary oxide systems B<sub>2</sub>O<sub>3</sub>–Al<sub>2</sub>O<sub>3</sub> reach a maximum activity at about 200 °C, which is by 50 °C lower than for Pt/Al<sub>2</sub>O<sub>3</sub>.

The temperature programmed reaction was performed in two subsequent tests. After the first catalytic test, the catalyst was subjected to thermal treatment at 400 °C, and then to the repeated test in TPR conversion of 1-butene. As follows from the plots in Fig. 5, the results of the second catalytic test are better than those of the first one, allowing a lower temperature of full 1-butene combustion. It seems



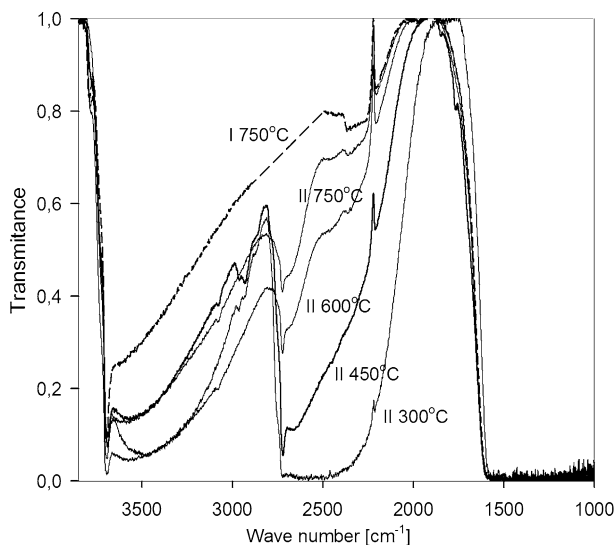


**Fig. 4** The effect of temperature on the dehydroxylation and desorption of  $D_2O$  for sample BAI 0.3. Experimental conditions: dehydroxylation ( $10^{-3}$  mmHg) 1 h 750 °C, adsorption of 10  $\mu$ l  $D_2O$ , desorption ( $10^{-3}$  mmHg) 0.5 h at 300 °C (II), 450 °C (II), 600 °C (II), 750 °C (II)

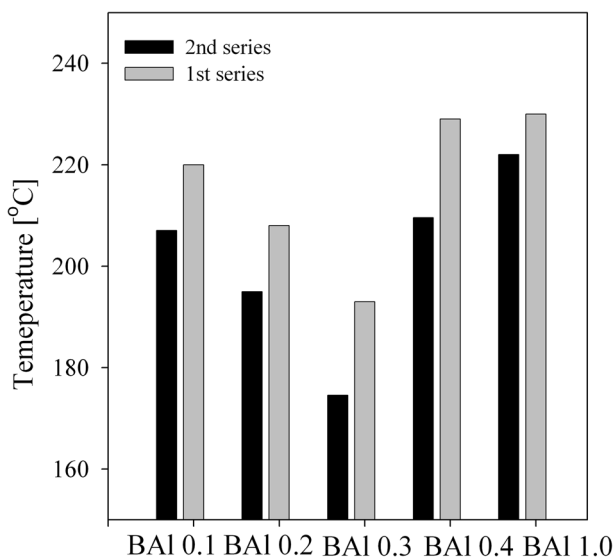


**Fig. 5** Temperature of the maximum conversion of 1-butene, ( $T_{max}$ ). Experimental conditions: Reaction gas–air, concentration of 1-butene  $2000 \pm 100$  ppm. Catalyst mass 60 mg, reactor ID = 6 mm. Reaction temperature ramp 20 °/min, range (35–400 °C)

that the presence of  $B_2O_3$  in the  $Al_2O_3$  matrix leads not only to a high degree of Pt dispersion but also limits the generation of  $PtO_x$  particles able to move on the support surface, so stabilizes the metal dispersion.

## Conclusions

The results presented have shown that modification of  $\text{Al}_2\text{O}_3$  with boron oxide is highly beneficial, not only because of the high dispersion values obtained but also because an increase in the content of  $\text{B}_2\text{O}_3$  does not reduce the dispersion but maintains it on a similar level. In the supports modified with  $\text{B}_2\text{O}_3$ , the high metal dispersion is not related to strong metal-support interactions, as e.g. in  $\text{SnO}_2$ , but the porous structure of the support that stabilizes small metal clusters on the surface. Another factor conducive to the stabilization of small clusters of Pt groups is the acidic character of the support surface caused by the presence of boron oxide. It seems that the old theory proposed by Boreskov [44] is confirmed by the results presented and perhaps it should play an important role in designing systems with nanometallic phase.

**Open Access** This article is distributed under the terms of the Creative Commons Attribution 4.0 International License (<http://creativecommons.org/licenses/by/4.0/>), which permits unrestricted use, distribution, and reproduction in any medium, provided you give appropriate credit to the original author(s) and the source, provide a link to the Creative Commons license, and indicate if changes were made.

## References

1. Flytzani-Stephanopoulos M, Gates BC (2012) *Annu Rev Chem Biomol Eng* 3:545–574
2. Tauster SJ, Fung CS (1978) *J Catal* 55:29–35
3. Tauster SJ, Fung SC, Garten RL (1978) *J Am Chem Soc* 100:170–175
4. Curtin T, McMonagle JB, Hodnett BK (1992) *Appl Catal A* 93:91
5. Izumi Y, Sato S, Urabe K (1983) *Chem Lett* 1649–1652
6. Werke L (1955) East Ger Patent 10920
7. Irnich R (1976) BASF Ger Patent 1227028
8. Immel O, de Jager A, Kaiser BU, Schwarz HH (1978) Bayer Jpn Patent S53-037686
9. Murakami Y, Saeki Y, Ito K (1972) *Nippon Kagakukaishi* 1:12
10. Sakurai H, Sato S, Urabe K, Izumi Y (1985) *Chem Lett* 1783–1784
11. Delmastro A, Gozzelino G, Mazza A, Vallino M, Busca G, Lorenzelli V (1994) *J Chem Soc* 90:2663
12. Wang WJ, Che YW (1991) *Che Catal Lett* 10:297
13. Peil K, Galya LG, Marcelin G (1989) *J Catal* 115:441
14. Engels S, Herold E, Lausch H, Mayr H, Meiners HW, Wilde M (1992) In: *Proceedings of the 10th international congress on catalysis*, p 2581
15. Murakami Y, Otsuka K, Wada Y, Morikawa A (1990) *Bull Chem Soc Jpn* 63:340
16. Cucinieri-Colorio G, Auroux A, Bonnetot B (1993) *J Term Anal* 40:1267
17. Cucinieri-Colorio G, Bonnetot B, Védrine JC, Auroux A (1994) New developments in selective oxidation II. In Cortés Corberán V, Vic Bellón S (eds), Elsevier Science Publishers, p 143
18. Colorio G, Védrine JC, Auroux A, Bonnetot B (1996) *Appl Catal A* 137:55
19. Buyevskaya OV, Kubik M, Baerns M (1996) Symposium on heterogeneous hydrocarbon oxidation presented before the division of petroleum chemistry, Inc., 211th national meeting, American Chemical Society, p 163
20. Pine L (1976) US Patent 3,993,557
21. Bailey WA (1945) US Patent 2,377,744
22. De Bataafsche NV (1949) Petroleum Maatschappij te's-Gravenhage Dutch Patent 62,287
23. De Bataafsche NV (1950) Petroleum Maatschappij te's-Gravenhage Dutch Patent 65,287
24. Sato S, Kuroki M, Sodesawa M, Nozaki T, Maciel GE (1995) *J Mol Catal* 104:171
25. Izumi Y, Shiba T (1964) *Bull Chem Soc Jpn* 37:1797

26. Tanabe K (1970) Solid acids and bases. Academic press, New York, p 131
27. Xiaoding X, Boelhouwer C, Benecke JI, Vonk D, Mol JC (1986) *J Chem Soc* 1(82):1945
28. Sibeijn M, van Veen JAR, Blik A, Moulijn JA (1994) *J Catal* 145:416
29. Chen YW, Li C (1992) *Catal Lett* 13:359
30. Okihara T, Tamura H, Misono MJ (1995) *J Catal* 95:41
31. Yazawa Y, Yoshida H, Tahagi N, Kagi N, Komai S, Satsuma A, Murakami Y, Hattori T (2000) In: 12th international congress on catalysis (*Stud Surf Sci Catal*, vol 130), p 2189
32. Kirszensztejn P, Szymkowiak A, Marciniak P, Martyła A, Przekop R (2003) *Appl Catal* 245:159–166
33. Kirszensztejn P, Przekop R, Szymkowiak A, Mackowska E, Gaca J (2006) *Microporous Mesoporous Mater* 89:150–157
34. Martyła A, Olejnik B, Kirszensztejn P, Przekop R (2011) *Int J Hydrog Energy* 36:8358–8364
35. Przekop R, Kirszensztejn P (2014) *J Non Cryst Solids* 402:128–134
36. Nowicki W, Rypka G, Kawałko A, Tolińska A, Kirszensztejn P (2014) *J Mater Sci* 49:4416–4422
37. Falconer JL, Schwarz JA, Catal J (1983) *Rev Sci Eng* 25:141–227
38. Kwak JH, Hu J, Mei D, Yi CH-W, Kim DH, Peden CHHF, Allard LF, Szanyi J (2009) *Science* 325:1670–1673
39. Ishihara T, Harada K, Eguchi K, Arai H (1992) *J Catal* 136:161
40. Yazawa Y, Takagi N, Yoshida H, Komai S, Satsuma A, Tanaka T, Yoshida S, Hattori T (2002) *Appl Catal A* 233:103–112
41. Alexeev OS, Graham GW, Shelef M, Gates BC (2000) *J Catal* 190:157
42. Cremaschi P, Whitten JL (1987) *Chem Mater Sci* 72:485
43. Minot C, Bigot B, Hariti A (1986) *J Am Chem Soc* 108:196
44. Borekov GK, Karnauchov AP (1952) *Ž F Ch* 26:26
45. Zou W, Gonzales RD (1993) *Appl Catal A* 102:181–200